Journal of Sound and Vibration (1999) **222**(4), 597–620
Article No. jsvi.1998.2064, available online at http://www.idealibrary.com on IDEAL

NON-LINEAR ANALYSIS OF COMPRESSIVELY/THERMALLY STRESSED ELASTIC SHELL STRUCTURES ON THE STEELPAN AND THE UNDERLYING THEORY OF THE TUNING PROCESS

A. ACHONG

Department of Physics, University of the West Indies, St Augustine, Trinidad, W.I.

(*Received* 8 *July* 1998, *and in final form* 23 *November* 1998)

This paper presents a non-linear analysis of the dome-shaped notes on the steelpan under compressive and thermal stresses. Equations are derived for the static and dynamic response of symmetrically distorted notes. Analytical results are obtained for modal frequencies, non-linear coupling coefficients and the buckling parameter. Experimental results demonstrate the vibration characteristics and their dependence on temperature. Experimental results were also obtained for the effects of stress relaxation which follows the shaping and tuning process of these notes by hammer peening. The results of the analysis are applicable to other shell-like structures not necessarily designed for musical purposes.

1. INTRODUCTION

The present study deals with some analytical and experimental results on the thin, shallow, domed-shaped notes found on the steelpan. The previous reports on the non-linear behaviour of these structures [1–3] made extensive use of quadratic modal coupling. This paper finds expressions for the quadratic and cubic coupling coefficients in terms of the geometrical and elastic parameters characterizing the notes. What is in fact interesting, indeed remarkable, is that this musical instrument makes effective use of the quadratic and cubic non-linearities of shells [4–6]. Panmakers have often used expressions such as "the pan has a life of its own" when confronted with the curious behaviour of this instrument during manufacture.

To avoid any misunderstanding, it is made clear that the non-linear formulations in this paper do not provide the panmaker with a formula into which numerical substitutions can be made for the calculation of note frequencies or the relative magnitudes of the partials. Indeed, rather more modest aims are set. The approach will be to begin with an elastically supported

0022–460X/99/190597 + 24 $30.00/0

spherical cap under compressive and thermal stresses, impose shape deformations on the cap to simulate the note-shaping process, and then solve the resulting non-linear dynamic equations to yield expressions for the modal frequencies and coupling coefficients. It will be shown that this approach provides explanations for a very broad range of effects observable on the pan during and after tuning.

The study relates to some of the problems of concern to the panmaker such as the enhancing of relative amplitudes of the partials on the instrument, harmonic tuning of the overtones, and the production, on a consistent basis, of notes with acceptable tonal characteristics. While the average panmaker may not have a background in applied dynamics or experimental testing, it is important that the factors characterizing the mechanisms of production of steelpan sound be properly documented. The results of the present study, when combined with the skills of the panmaker, can have significant musical consequences including the generation of strong partials, purity of tuning and providing rules for adjusting eigenmodes and modal couplings.

2. NOTE PREPARATION AND DYNAMIC BEHAVIOUR

In order to develop a consistent and applicable theoretical model for the steelpan notes it is necessary to consider the preparation of these shell-like steel structures. Each note forms a sub-structure of a complex array of similarly prepared shallow shells over the indented face of a steel drum [1]. The structure

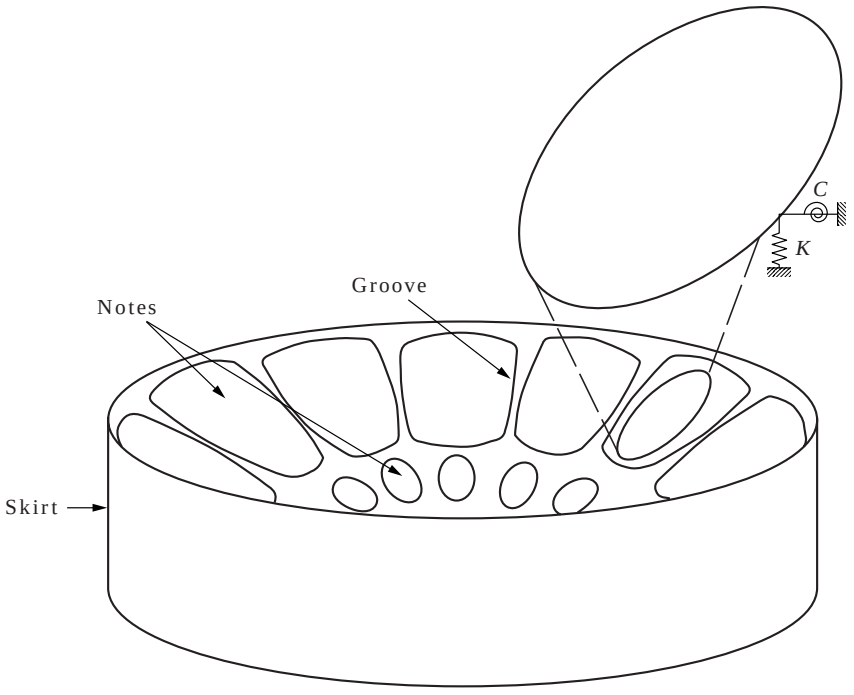

Figure 1. Typical arrangement of notes on the face of a tenor steelpan. The elliptical area of mode localization is shown enlarged and elastically supported.

of these notes, depicted in Figure 1, differ only in the details that give each note its particular frequency and position on the musical scale. The family of steelpans include the high-range *tenor*, the mid-range *cello* and the low-range *bass*. Pans such as the *double second*, the *guitar* and others, fill in, to cover (with overlap) the musical range from G_1 (48·999 Hz) to F_6 (1396·9 Hz).

2.1. PEEN-FORMING, ANNEALING, TUNING AND CHROMING

In the manufacture of the steelpan, one face of a steel drum is indented to a centre-depth dependent on the type of instrument required—tenors are indented to a depth of approximately 18 cm while the corresponding depth for the bass is around 10 cm. The shaping of the panface is achieved by the peening action of a hammer applied to the top surface. The cylindrical side of the drum is cut to a length consistent with the musical range of the instrument—this skirt-length is typically around 20 cm on the tenor and full length (56 cm) on the bass. The raised notes are then made by peening and shaping from the underside.

The shaped pan is then subjected to a low-temperature *stress relief annealing* process by heating to a temperature T_a ($T_a < T_e - 170°\mathrm{C}$, where T_e is the eutectoid temperature of the steel) for 20 to 30 min, followed by immersion in or dousing with water. This is designed to reduce the effects of cold working (peening) without affecting the mechanical properties of the partially finished panface. Higher temperatures may completely eliminate the strain hardening achieved on cold working, resulting in a material that is too soft for use on a percussion instrument. The treated notes are then tuned (*first-tuning*) by a more controlled shaping and peening action with the hammer.

It has become common practice today, after *first-tuning*, to chrome the higher frequency pans and to retune afterwards (*second-tuning*). Chroming is done mainly for aesthetics and to reduce rusting.

2.2. BOUNDARY CONDITIONS AND INTERNAL STRESSES

The hammer peening to indent the panface and to form or tune the notes, like shot-peening [7] or ball forming [8], induce residual compressive stresses in the material which are partially reduced and redistributed by tempering. The evidence for the existence of these residual compressive stresses on the steelpan, comes directly from the observations of two effects [9].

The first is the (infrequent) occurrence of *localized buckling* in small areas of the note (usually around 2 cm across) during the tuning process. This effect, termed "*flapping*" for the "paper-like" behaviour displayed by the affected area, is the first of the "curious behaviour" observed by the panmaker. Localized buckling is produced by the excessive compressive stresses in the region of interest and the resulting reduction (to zero) of the effective dynamic stiffness.

The second effect is the small upward shift in the frequency of the notes after the newly completed pans are made (the second "curious behaviour"). This tendency to "*run sharp*" is observable (to the trained ear) just one day after manufacture and the frequency shift may slowly increase during the first week.

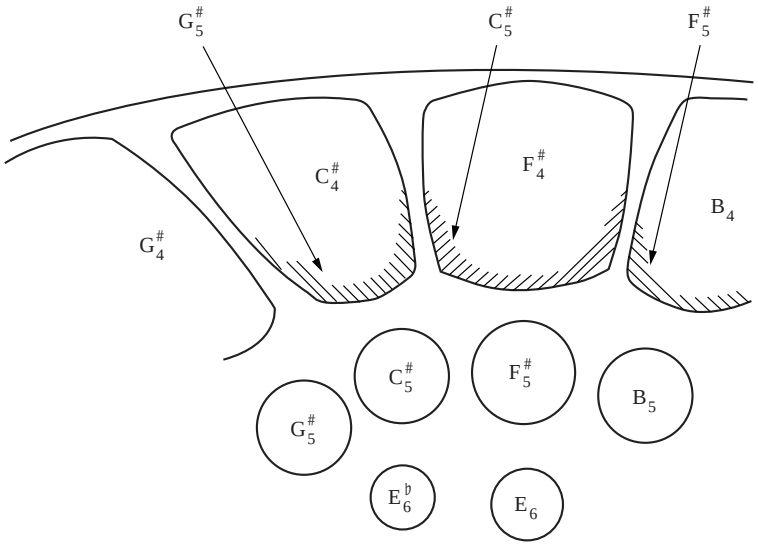

Figure 2. Details of note arrangement showing musical tones that may be excited on the panface.

This shift has been interpreted by the author as a direct result of the reduction in residual compressive stresses through stress relaxation.

Each note, by its connection to the rest of the panface, will be characterized by a set of hidden boundary conditions describing the note edges, and by unknown residual (compressive) stresses. The usual procedure of separating the edge supports into independent translational and rotational springs (see Figure 1) as suggested by Achong [1] for the areas of localization, although possible in principle, may not be easily achieved in practice, where, as expected, it will not be possible to independently vary or control each of these two elastic parameters. In practice it is found that it is not required that the stiffness be constant along the boundary. In fact, panmakers, on purpose, create variations in edge supports when for example, sections (or separate domains) of the same note are tuned to different frequencies. This is illustrated in Figure 2. In cases where the notes are tuned in the manner indicated in Figure 2, *domain interaction* [2] is deliberately incorporated into the note dynamics.

As an all-metal instrument, thermal stresses will also play an important role in the system dynamics. With just a few degrees change in temperature, noticeable changes occur to the frequencies of the notes. Temperature changes can also affect the tonal structure by modifying the relative amplitudes of the partials as well as the amplitude and frequency modulations.

2.3. OBSERVATIONS

Achong [1, 10] has reported the confinement (mode localization) of the vibratory motion of a note, to an elliptical region defined within the area bordered by the groove (see Figure 1). The grooves are not essential [1] although they assist in blocking the note to reduce inter-note coupling. Investigation by

the author of many types of steelpans (tenors, seconds, cellos etc.) gives a mean aspect ratio of $1{\cdot}27 \pm 0{\cdot}08$ for the elliptical planform defining the area of localization. The peening action applied during tuning is carefully applied to the boundary that defines this area.

Achong [1] has given unmistakable evidence for the non-linear nature of the vibratory modes excited within these areas of localization, by showing the occurrence of the jump phenomenon and Hopf bifurcation on a properly tuned note of a tenor pan. This type of behaviour can be observed on notes that show strong coupling between the first two modes and has also been shown by Achong [1] to be a direct consequence of quadratic non-linearity on these shell-like structures.

It has been found that the second mode can only be of significant intensity when the corresponding linear frequency is approximately twice the linear frequency of the first mode. The systems therefore possess internal resonances (i.e., they are systems with commensurate linearized natural frequencies). When the second mode to first mode frequency ratio is (typically) within $2 \pm 0{\cdot}006$, quadratic couplings are strong, resulting in deep amplitude and frequency modulations [1, 2] and account for the distinctive tonal structure of the instrument.

Notes that display a relatively weak second mode tend to display more rapid, low level, amplitude (and frequency) modulations. They also show a somewhat larger departure from harmonicity (second mode typically at the end of the range $2 \pm 0{\cdot}02$). Notes produced with these weak mode-coupling characteristics, however, lack the musical lustre and colour of notes with strong couplings.

King and Vakakis [11] developed an energy-based methodology for non-linear resonant modal interactions and in applying the method to a "3:1" resonance on a hinge–clamped beam have shown that the response of the non-resonant functions are minimal in comparison with the resonant mode. This result which is qualitatively in agreement with the observations made on the steelpan would suggest the occurrence of these resonances in a wider variety of engineering and musical systems (the Chinese gong for example).

For variations on a pan, good panmakers create a mixture of notes with varying degrees of mode coupling (although they lack the understanding of this non-linear process).

3. NON-LINEAR ANALYSIS

3.1. THE BASIC SHELL STRUCTURE

In the analysis that follows, the non-linear dynamics are developed for the shell-like region where the motion is localized, as shown in Figure 1. This region is assumed as having a basic spherical form which can then be distorted into the desired shape. While this procedure is not necessary, the strategy leads to some convenience in the development, especially as it would be desirable to incorporate the tuning process in which the notes are changed from one shape to another. In addition to this, the "rise" is a readily noticeable feature of the

dome-shaped notes. It would therefore be beneficial to regard the rise as a *distinguished parameter* and to keep it separated from other parameters defining the shape (or form) of the shell. By not concealing the rise within some general shape-function, some aspects of the role played by this physically meaningful parameter may be determined even without completely solving the final equations.

In the present analysis, a completely satisfactory description of the problem is obtained by restricting the analysis to regions displaying axisymmetric properties on a circular planform (recall that the mean aspect ratio is 1·27, not too far from unity). While this restriction has the effect of removing the aspect ratio as a tuning parameter, it still allows the note dynamics to be fully studied.

The shell geometry is depicted in Figure 3. R is the mid-surface radius (with $R = R_0 =$ constant, when the form is perfectly spherical), a is the planform radius, H_0 is the rise, and h (not shown) is the thickness. It will be convenient to define the ratio H_0/h as the "*rise factor*". W, u_ϕ and u_θ are, respectively, the transverse, azimuthal and radial displacements, and are functions of the space co-ordinates and time. Since only axisymmetric deformations are considered, all displacements and stresses are independent of the variable ϕ and $u_\phi = 0$. A position co-ordinate r is defined as $r = R \sin \theta$. As shown in reference [10], the relative dimensions of these structures satisfy the criteria for treatment as shallow shells.

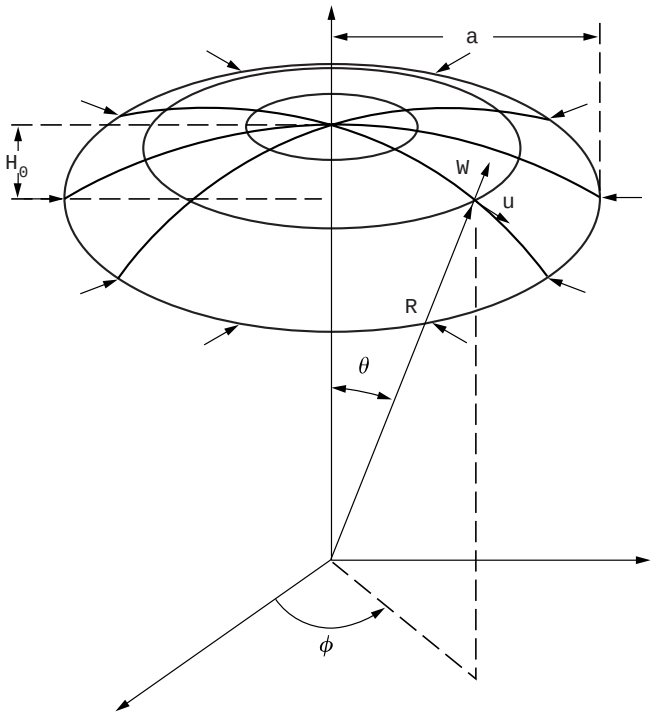

Figure 3. Shell geometry.

The analysis begins with the basic shell equations given by Connor [12] and by Grossman *et al.* [6] for the axisymmetric motion of a thin homogeneous spherical shell (in dimensionless form):

$$\frac{1}{12}\nabla^4 W + 2(1+\nu)\left(\frac{a}{2R_0}\right)\left(\frac{a}{h}\right)^2\left[\left(\frac{\partial}{\partial x}+\frac{1}{x}\right)u + 4\left(\frac{a}{2R_0}\right)W\right] + (1+\nu)\left(\frac{a}{h}\right)\left(\frac{a}{2R_0}\right)\left(\frac{\partial W}{\partial x}\right)^2 - \left(\frac{a}{h}\right)\left(\frac{\partial}{\partial x}+\frac{1}{x}\right) \times \left[\frac{\partial W}{\partial x}\left(\frac{\partial}{\partial x}+\frac{\nu}{x}\right)u + 2(1+\nu)\left(\frac{a}{2R_0}\right)W\frac{\partial W}{\partial x} + \left(\frac{h}{2a}\right)\left(\frac{\partial W}{\partial x}\right)^3\right] + \frac{\partial^2 W}{\partial \tau^2} = 0, \tag{1a}$$

$$\frac{\partial}{\partial x}\left(\frac{\partial}{\partial x}+\frac{1}{x}\right)u + 2(1+\nu)\left(\frac{a}{2R_0}\right)\frac{\partial W}{\partial x} + \left(\frac{h}{2a}\right)\left(\frac{\partial}{\partial x}+\frac{1-\nu}{x}\right)\left(\frac{\partial W}{\partial x}\right)^2 = 0, \tag{1b}$$

where $u(x, \tau)$ and $W(x, \tau)$, in units of shell thickness h, are the radial and transverse displacements respectively, $x = r/a$, $\nabla^4 = (\partial^2/\partial x^2 + (1/x)\partial/\partial x)^2$, $\tau = \gamma t$, $\gamma^2 = Eh^2/[\rho a^2(1-\nu^2)]$, with E being Young's modulus, ρ the shell density and ν denotes Poisson's ratio. Equation (1a) represents the dynamical equilibrium condition for the forces acting on an infinitesimal element of the shell while equation (1b) is the compatibility condition for the displacement fields $u(x, \tau)$ and $W(x, \tau)$. Equations (1) include the first order effects of bending and stretching, but contain no rotatory (torsional) or longitudinal inertia terms.

If the edge of the shell is fixed in the longitudinal direction and elastically supported by translational and rotational springs having, respectively, distributed stiffness K (N/m^2) and C (Nm/m) (as in Figure 1), the necessary boundary conditions are

$$[u]_{x=1} = 0, \quad C\left[\frac{\partial W}{\partial x}\right]_{x=1} = -\frac{D}{a}\left[\frac{\partial^2 W}{\partial x^2} + \frac{\nu}{x}\frac{\partial W}{\partial x}\right]_{x=1}, \qquad K[W]_{x=1} = \frac{D}{a^3}\left[\frac{\partial}{\partial x}\left(\frac{\partial^2 W}{\partial x^2} + \frac{1}{x}\frac{\partial W}{\partial x}\right)\right]_{x=1}, \tag{2a–c}$$

where D is the flexural rigidity defined as $D = Eh^3/12(1-\nu^2)$. In general, K and C may not be constant along the edges but to retain the axisymmetric nature of the analysis, their constancy is required. For the clamped edge, $C = \infty$, $K = \infty$, making $[\partial W/\partial x]_{x=1} = 0$, $[W]_{x=1} = 0$.

By symmetry, the following conditions hold at the pole:

$$[u]_{x=0} = 0, \quad [\partial W/\partial x]_{x=0} = 0. \tag{3a, b}$$

3.2. FORCED OSCILLATIONS AND STICK IMPACTS

Forced oscillations (for steady state or bifurcation studies) are considered by including a harmonically applied surface load that is symmetrical about the pole and normal to the surface. Stick impacts may also be considered by including a short duration surface load applied normal to the surface over an area (the contact area) $\delta A = \pi b^2/4$ where b is the stick-width. To maintain the symmetry of the motion being considered here, the mid-impact point must be at the pole (in the terminology of the pannist, this point on the note is referred to as the "*sweet-spot*"). The general form of the load can be written as $z(x)p(\tau)$, where $z(x)$ is a shape function describing the distribution of the applied load over the surface and $p(\tau)$ is a sinusoidal function for harmonic loading or a pulse for stick impacts. The forcing term to be added to the right-hand side of equation (1) is therefore $\check{z}(x)p(\tau)$, where

$$\check{z}(x) = \frac{(1-\nu^2)}{E}\left(\frac{a}{h}\right)^4 z(x).$$

For harmonic loading,

$$p(\tau) = \sin(\Omega\tau), \tag{4}$$

where $\Omega = \omega/\gamma$ with ω as the external driving frequency. On the steelpan, sinusoidal excitation may be applied acoustically or by attaching an electromagnetic vibrator at some point remote from the note being excited.

For stick impacts, the force–time history $p(\tau)$ can be modelled by a half-sine function

$$\begin{aligned} p(\tau) &= \sin(\pi\tau/\tau_c), \quad 0 \leqslant \tau \leqslant \tau_c, \\ &= 0, \qquad\qquad\quad \text{otherwise}, \end{aligned} \tag{5}$$

where $\tau_c = \gamma t_c$ with t_c as the *contact-time*. If the applied force is assumed to be uniform over the area δA, then one has

$$\begin{aligned} z(x) &= 1, \quad |x| \leqslant \frac{1}{2}\left(\frac{b}{a}\right), \\ &= 0, \quad |x| > \frac{1}{2}\left(\frac{b}{a}\right). \end{aligned} \tag{6}$$

3.3. VISCOUS DAMPING

Since the dynamic equations will prove to be non-linear, implying the possibility of internal resonances, the shell material may be subjected to several frequencies at the same time. In the analysis by Achong [3], the damping coefficient μ was assumed to be independent of frequency and therefore the same for each excited mode. Not only was this assumption confirmed experimentally [3], it also proved to be effective in allowing the integration of the non-linear

equations to proceed. The inclusion of viscous damping adds to the left-hand side of equation (1a) the term $+\breve{\mu}\partial W/\partial\tau$, where $\breve{\mu} = \mu\gamma(1-\nu^2)a4/(Eh^3)$ with μ as the damping coefficient. It should be noted that the damping coefficient is a temperature dependent parameter.

3.4. COMPRESSIVE AND THERMAL STRESSES

The next modification is the inclusion of a uniform compression $-N_c$ (N/m) applied radially along the shell boundary. This adds a constant in-plane stress σ_c $(=-N_c/h)$ to the stress components $\sigma_{\theta\theta}$ and $\sigma_{\phi\phi}$, which in turn introduces to the left-hand side of equation (1a) the extra terms $+\breve{N}_c\nabla^2 W - 2\breve{N}_c a^2/(hR)_o)$ (see, for example, reference [13]), where $\breve{N}_c = N_c a^2(1-\nu^2)/Eh^3$.

For this all-steel instrument, it is reasonable to assume uniform temperature (and uniform temperature change) over the area of a single note. Because of the small thickness of the material (around 0·3 mm) one can also assume that the temperature does not vary through the shell thickness. Thermally induced shear forces therefore do not arise.

For a uniform temperature rise δT the affected shell stress–strain relations (including the effects of compression) are

$$\sigma_{\theta\theta} = \frac{E}{(1-\nu^2)}\left[\varepsilon_{\theta\theta} + \nu\varepsilon_{\phi\phi} - (1+\nu)\alpha\delta T\right] + \sigma_c,$$
$$\sigma_{\phi\phi} = \frac{E}{(1-\nu^2)}\left[\varepsilon_{\phi\phi} + \nu\varepsilon_{\theta\theta} - (1-\nu)\alpha\delta T\right] + \sigma_c, \qquad (7a, b)$$

where α is the thermal expansion coefficient. These stress-strain relations lead to simple expressions for the thermally induced in-plane stress resultants $N_{\theta\theta} = N_{\phi\phi} = hE\alpha\delta T/(1-\nu)$. As in the case of in-plane compressive loading, thermal loading will produce two additional terms on the left-hand side of equation (1a). These terms are $+\breve{N}_T\nabla^2 W - 2\breve{N}_T a^2/(hR_0)$, where $\breve{N}_T = \alpha\delta T(1+\nu)(a/h)^2$.

Combining the effects of in-plane loading and uniform temperature rise, the modification to equation (1) is the addition of the terms $+(\breve{N}_c + \breve{N}_T)\nabla^2 W - 2(\breve{N}_c + \breve{N}_T)a^2/(hR_0)$. This result for the combined effects can be obtained directly by making use of the "body-force analogy" [14]. One immediately observes from this result that temperature changes will produce effects identical to those observed for changes in the compressive forces.

3.5. DEFORMED SHELL

Consider now the shell to be deformed symmetrically about the pole such that $R = R_0 + q(x)\cdot H_0$, where $q(x)$ is an imperfection function representing a small (dimensionless) distortion of the shell mid-surface and $H_0 = a^2/2R_0$. Along the boundary of the shell, $q(1) = 0$. The radius of curvature R_c of the mid-surface of this deformed shell will vary with the angle θ:

$$\frac{1}{R_c} = \frac{R^2 + 2(\mathrm{d}R/\mathrm{d}\theta)^2 - R(\mathrm{d}^2R/\mathrm{d}\theta^2)}{[R^2 + (\mathrm{d}R/\mathrm{d}\theta^2]^{3/2}}. \tag{8}$$

Since $q(x) \cdot H_0 \ll R_0$, by dropping all terms higher than first order in $q(x) \cdot H_0/R_0$, the quotient $Q(x)$ $(= R_0/R_c)$, to be referred to here as the *surface imperfection*, can be defined:

$$Q(x) = 1 - 2\left(\frac{H_0}{a}\right)^2 q - \frac{1}{2}\frac{\mathrm{d}^2 q}{\mathrm{d}x^2}. \tag{9}$$

On the notes of the steelpan, the ratio H_0/a takes values typically around 1/40 [10], so that the second term in $Q(x)$ may be relatively small. For the deformed shell, the variable curvature $Q(x)/R_0$ replaces $1/R_0$ in the development of the new equations to replace the perfect shell equations (1a,b).

3.6. EXTENDED DYNAMIC EQUATIONS

By including forcing, damping, in-plane loading, temperature change and shell deformation into the system of non-linear dynamic equations, the new set of equations are

$$\begin{aligned}
&\frac{1}{12}\nabla^4 W + 2(1+\nu)\left(\frac{a}{2R_0}\right)\left(\frac{a}{h}\right)^2\left[Q\left(\frac{\partial}{\partial x} + \frac{1}{x}\right)u + 4\left(\frac{a}{2R_0}\right)Q^2 W\right] \\
&\quad + (1+\nu)\left(\frac{a}{h}\right)\left(\frac{a}{2R_0}\right)\left(\frac{\partial W}{\partial x}\right)^2 Q - \left(\frac{a}{h}\right)\left(\frac{\partial}{\partial x} + \frac{1}{x}\right) \\
&\quad \times \left[\frac{\partial W}{\partial x}\left(\frac{\partial}{\partial x} + \frac{\nu}{x}\right)u + 2(1+\nu)\left(\frac{a}{2R_0}\right)QW\frac{\partial W}{\partial x} + \left(\frac{h}{2a}\right)\left(\frac{\partial W}{\partial x}\right)^3\right] \\
&\quad + (\breve{N}_c + \breve{N}_T)\nabla^2 W - 2(\bar{N}_c + \bar{N}_T)\left(\frac{a^2}{hR_0}\right)Q + \frac{\partial^2 W}{\partial \tau^2} + \breve{\mu}\frac{\partial W}{\partial \tau} = \breve{z}(x)\rho(\tau),
\end{aligned} \tag{10a}$$

$$\frac{\partial}{\partial x}\left(\frac{\partial}{\partial x} + \frac{1}{x}\right)u + 2(1+\nu)\left(\frac{a}{2R_0}\right)Q\frac{\partial W}{\partial x} + \left(\frac{h}{2a}\right)\left(\frac{\partial}{\partial x} + \frac{1-\nu}{x}\right)\left(\frac{\partial W}{\partial x}\right)^2 = 0. \tag{10b}$$

4. STATIC AND DYNAMIC STATES

4.1. TRI-MODAL SOLUTION OF THE NON-LINEAR EQUATIONS

On inspecting equations (10) one clearly sees the appearance of linear, quadratic and cubic terms in the displacement $W(x, \tau)$. This means that in addition to the natural modes at frequencies ω_n ($n = 1, 2, 3, \ldots$), components at $m\omega_n$ ($m = 2, 3$) and at combination frequencies will be present. However, the

panmaker can tune the notes to ensure the close harmonicity of the natural modes $\omega_n \approx n\omega_1$, thereby achieving a reduction in the number of spectral components and setting the conditions necessary for the generation of internal resonances. While it would be possible to obtain a solution involving all the spectral components, for the purposes of the present work, the lead taken by the panmaker will be followed by applying the condition $\omega_n \approx n\omega_1$, $n = 2, 3, \ldots$.

Experimental results in reference [1] show that for the steelpan, only the first three (and occasionally four) frequency components are of sufficient amplitudes to be of musical interest. Therefore, in order to solve equation (1x) for the deflection, it will be assumed that the variable $W(x, \tau)$ may be expressed in separable form as the sum of a space-dependent function representing the static state and three space and time-dependent functions representing the dynamic state of the system. Thus, one can write the truncated series expansion

$$W(x, \tau) = \psi_0 + \sum_{i=1}^{3} \psi_i(x) w_i(\tau), \tag{11}$$

where the modal co-ordinates (mode shapes) ψ_i ($i = 1, 2, 3$) and static state ψ_0 must satisfy both the boundary conditions in equation (2) and the conditions at the pole (equations (3a, b)), the modal co-ordinates $W_i(\tau)$, are unspecified functions of time to be determined. Higher modes ($n > 3$), *by assumption*, do not, contribute significantly to the system response.

When $W(x, \tau)$ is substituted from equation (11), equation (10b) is solved for $u(x, t)$ by successive integration and by employing the conditions of equations (3a, b). Using this solution for $u(x, t)$ in equation (10a), performing the conventional Galerkin averaging (premultiplying equation (10a) by the ith modal function and integrating from $x = 0$ to $x = 1$) and consolidating terms (see Appendix A), yield the equations for the dynamic state. The static state is extracted during this analysis before the Galerkin procedure is applied. The functionals L, M, P, S, V, X, Y and Z which appear in these equations are defined in Appendix A. In deriving the coupling parameters in the dynamic equations, close harmonicity $\omega_n \approx n\omega_1$ is assumed.

4.2. THE STATIC STATE

The static equation describing the dimensionless surface displacement $\psi_0(x)$, produced by compressive and thermal stresses is given by

$$\frac{1}{12}\nabla^4\psi_0 + 8(1+\nu)\left(\frac{H_0}{h}\right)^2\left\{Q^2\psi_0 - \frac{1}{2}(1+\nu)P(Q\psi_0', Q)\right\} - (\breve{N}_c + \breve{N}_T)\nabla^2\psi_0$$
$$+ (1+\nu)\left(\frac{H_0}{h}\right)\{S(\psi_0'^2, Q) + Q\psi_0'^2 + 2Y(\psi_0', Q\psi_0') - 2V(Q\psi_0\psi_0')\}$$
$$+ \frac{1}{2}Z(\psi_0', \psi_0'^2) + \frac{1}{2}V(\psi_0'^3) + 4(\breve{N}_c + \breve{N}_T)\left(\frac{H_0}{h}\right)Q = 0, \tag{12}$$

where $(\cdot)' = \mathrm{d}(\cdot)/\mathrm{d}x$. The special case of $(\breve{N}_c + \breve{N}_T)(H_0/h) = 0$, arising when the

compressive and thermal stresses are zero or the note surface is flat ($H_0 = 0$), has the trivial solution $\psi_0 = 0$.

The shape of the stressed note is described by the radius

$$R(x) = R_0 + q(x)H_0 + \psi_0(x)h. \tag{13}$$

Equation (13) shows that the equilibrium shape of the note is dependent on both the form imposed by the panmaker in shaping the note (the $R_0 + q(x)H_0$ terms) and that induced by the stresses (the $\psi_0(x)h$ term). In practice, it will not be possible to separate these two contributions by direct measurement. From equation (13), it is clear that note shapes are determined not only by the panmaker but also by the underlying mechanism (dependent on in-plane compressive forces and thermal stresses) that controls the static equilibria of these shell structures. This gives a partial explanation to the panmaker's observation that the pan appears to have "a life of its own". This is an effect that can be minimized but not removed entirely because of the shell-like geometry of the notes.

4.3. THE DYNAMIC STATE

If the external force $p(\tau)$ is resolved into its temporal Fourier components $F_n(p(\tau))$, the modal equations derived from equations (10a, b) are a set of second-order ODEs given by

$$\frac{\mathrm{d}^2 w_n}{\mathrm{d}\tau^2} + \mu_n \frac{\mathrm{d}w_n}{\mathrm{d}\tau} + \omega_n^2 w_n + \sum_{i,j=1}^{3} \alpha_{jk,n} w_j w_k + \sum_{i,j,k=1}^{3} \beta_{ijk,n} w_i w_j w_k = p_n, \quad (n = 1, 2, 3), \tag{14}$$

where $\mathrm{d}^2 w_n/\mathrm{d}\tau^2$ is the inertial term, $\mu_n \, \mathrm{d}w_n/\mathrm{d}\tau$ represents viscous damping ($\mu_n \doteq \breve{\mu}$), $\omega_n^2 w_n$ is the usual structural stiffness term (which includes the effects of thermal and compressive stresses), $\sum_{i,j=1}^{3} \alpha_{jk,n} w_j w_k$ represent quadratic stiffness, $\sum_{i,j,k=1}^{3} \beta_{ijk,n} w_i w_j w_k$ represents the cubic stiffness, and the p_n are the modal external forces, with

$$p_n = F_n(p(\tau)) \left(\int_0^1 \breve{z}(x) \psi_n x \, \mathrm{d}x \right) \Big/ \left(\int_0^1 \psi_n^2 x \, \mathrm{d}x \right). \tag{15}$$

The modal equations are coupled by the non-linear terms with coefficients $\alpha_{ij,n}$ and $\beta_{ijk,n}$.

The method of multiple scales [15, 16] may be used to construct a uniformly valid, asymptotic expansion of the modal equations, as done by Achong [1, 3] where only the quadratic (even-order) couplings are retained.

The procedure for obtaining numerical solutions for ψ_0 and ψ_n, and the corresponding eigenfrequencies ω_n, will involve lengthy iterations and extensive use of differential equation solvers. Although this problem is not a part of the present work, one may add that in solving for the eigenfrequencies corresponding to trial values for the spring constants K and C, it would be necessary to define detuning parameters σ_n (where $\omega_n = n\omega_1 \pm \sigma_n$). As explained

in references [1–3], the detuning parameters determine the tonal structure of a sounded note.

4.4. SMALL-DISPLACEMENT MODAL FREQUENCIES

The modal frequencies ω_n are given by the equation

$$\omega_n^2 = \frac{1}{12}\bar{L}_n(\psi_n) + 8(1+\nu)\left(\frac{H_0}{h}\right)^2\left\{\bar{M}_n(Q^2\psi_n) - \frac{1}{2}(1+\nu)\bar{P}_n(Q\psi'_n, Q)\right\}$$
$$- (\breve{N}_c + \breve{N}_T)\bar{X}_n(\psi_n) + 2(1+\nu)\left(\frac{H_0}{h}\right)\{\bar{Y}_n(\psi'_0, Q\psi'_n) + \bar{Y}_n(\psi'_n, Q\psi'_0)$$
$$+ \bar{M}_n(Q\psi'_0\psi'_n) - \bar{S}_n(\psi'_0\psi'_n, Q) - \bar{V}_n(Q\psi_0\psi'_n) - \bar{V}_n(Q\psi_n\psi'_0)\}$$
$$- \frac{3}{2}\bar{V}_n(\psi'_n\psi'^2) + \frac{1}{2}\bar{Z}_n(\psi'_n, \psi'^2_0) + \bar{Z}_n(\psi'_0, \psi'_0\psi'_n). \tag{16}$$

The modal frequencies ω_n are seen to depend on (1) the compressive and thermal stresses through the term with $(\breve{N}_c + \breve{N}_T)$ as a factor and through the terms involving the static displacement ψ_0, (2) the rise-factor (H_0/h) and surface imperfection (Q), both of which are parameters that are varied during tuning, and (3) the modal co-ordinates ψ_n which incorporate the spring constants on the note boundary. Generally, the frequencies will increase with the rise-factor. If the imperfection function Q tends to increase the overall curvature of the note, the frequencies may increase. Grossman *et al.* [6] have analyzed the case for perfectly spherical caps (for which $Q = 1$ and $\bar{M}_n(Q^2\psi_n) = 1$) under zero compressive and thermal stresses $(\breve{N}_c = 0 = \breve{N}_T)$, to obtain the first three terms of equation (16).

Using equation (16), one can explain the operation of an unorthodox method used by panmakers to tune the instrument. Since the effect of reducing the compressive stress $\breve{N}_c$ in equation (16) is an increase in frequency ($\delta\omega_n \propto -\delta\breve{N}_c$ for sufficiently small stress changes), fine tuning of the instrument can be done by heating individual notes with a blowtorch then allowing the notes to cool naturally to ambient temperature. Localized heating will produce a redistribution and reduction of the residual compressive stresses (*stress-relieving*). After cooling, when the treated note is sounded, there will be a clearly discernable "sharpening" of the tone.

When this procedure is taken together with the initial peening, shaping and tempering of the pan, one sees that the final tuned state (characterized by frequency) of an individual note, can be arrived at through infinitely many different ways. It can be said therefore, that *the tuned state has a history*. The conclusion is that the modal frequencies are not uniquely determined by the note geometry and the spring constants (K and C) defining the boundary. The same conclusion was arrived at in reference [10].

Since ω_n is dimensionless, the small-amplitude modal frequencies f_n in Hertz can be found from

$$f_n = \frac{\omega_n}{2\pi}\sqrt{\frac{Eh^2}{\rho a^4(1-\nu^2)}} \tag{17}$$

Unlike the small-amplitude frequencies defined above, the non-linear (large amplitude) frequencies are functions of time (being dependent on the modal interactions) and must be determined dynamically from the time derivative of the phases [1]. In general these non-linear sounding frequencies will not be equal to f_n because of the *pitch glides* and modulations [1] that characterize the tones of the steelpan.

4.5. BUCKLING

If the small-amplitude frequency for the first mode under the condition of zero compressive and thermal stresses is defined as ω_{10}, a buckling parameter s can be defined as

$$s = (\breve{N}_c + \breve{N}_T)\frac{\bar{X}_1(\psi'_1)}{\omega_{10}^2} + \frac{B(\psi_0)}{\omega_{10}^2}, \tag{18}$$

where $B(\psi_0)$ is the negative of the sum of all terms in ψ_0 appearing in equation (16). For the stressed note, the first mode small amplitude frequency can then be written as

$$\omega_1 = \omega_{10}(1-s)^{1/2}. \tag{19}$$

Buckling then occurs for $s = 1$, in which case the lowest mode frequency is reduced to zero as the global thermal expansion and/or compressive stress cancels out the structural stiffness for w_1 [17, 18]. Such cancellation can be observed in small regions on the note area but is not allowed to occur over the entire note. The panmaker can correct this compressive stress-induced buckling (“flapping”) by peening (“stretching”) the regions slightly away from the affected area. Proper stress-relief tempering during manufacture can reduce the tendency to buckle.

4.6. COUPLING COEFFICIENTS

In order to consolidate coefficients formed by the permutation of the subscripts on $\alpha_{jk,n}$ and $\beta_{ijk,n}$ (not including the mode designator, n) an asterisk will be used; for example, $\alpha^*_{jk,n} = \alpha_{jk,n} + \alpha_{kj,n}$.

4.6.1. *Square term coefficients*

The coefficient for the only term of the form $\alpha_{jj,n}w_j^2$ (the quadratic interaction of mode j with itself), is found in mode 2 for $j = 1$, and is given by

$$\alpha_{11,2} = 2(1+\nu)\left(\frac{H_0}{h}\right)\left\{\bar{Y}_2(\psi_1', Q\psi_1') + \frac{1}{2}\bar{M}_2(Q\psi_1'^2) - \frac{1}{2}\bar{S}_2(\psi_1'^2, Q) - \bar{V}_2(Q\psi_1\psi_1')\right\}$$
$$-\frac{3}{2}\bar{V}_2(\psi_0'\psi_1'^2) + \bar{Z}_2(\psi_1, \psi_0'\psi_1') + \frac{1}{2}\bar{Z}_2(\psi_0', \psi_1'^2). \tag{20}$$

It was shown in references [1–3] that this coupling coefficient plays a key role in determining the amplitude of the second mode as it controls the energy transferred from mode 1 to mode 2 via internal resonance. In the limit $H_0 \to 0$, as the shell tends towards the flat plate, the terms with H_0/h as a prefactor will be reduced to zero and the remaining terms will vanish because, in the case of the flat plate, $\psi_0 = 0$. On these dome-shaped notes, the rise-factor H_0/h will therefore be the main parameter controlling the $\alpha_{11,2}$ coefficient for the second mode. The effects of temperature and compressive stresses are introduced through the dependence on ψ_0'.

4.6.2. *Cross-term coefficients*

The coefficients $\alpha^*_{12,1}$, $\alpha^*_{23,1}$ (mode 1), $\alpha^*_{13,2}$ (mode 2), and $\alpha^*_{12,3}$ (mode 3), for cross terms of the form $\alpha^*_{jk,n} w_j w_k$ are given by

$$\alpha^*_{jk,n} = 2(1+\nu)\left(\frac{H_0}{h}\right)\{\bar{Y}_n(\psi_j', Q\psi_k') + \bar{Y}_n(\psi_k', Q\psi_j') + \bar{M}_n(Q\psi_j'\psi_k')$$
$$-\bar{S}_n(\psi_j'\psi_k', Q) - \bar{V}_n(Q\psi_j\psi_k') - \bar{V}_n(Q\psi_k\psi_j')\} + \bar{Z}_n(\psi_j', \psi_0'\psi_k')$$
$$+\bar{Z}_n(\psi_k', \psi_0', \psi_j') + \bar{Z}_n(\psi_0', \psi_j'\psi_k') - 3\bar{V}_n(\psi_0', \psi_j'\psi_k'), \quad (j \neq k). \tag{21}$$

These coupling coefficients determine the energy transfers; from mode 2 back to mode 1 ($\alpha^*_{12,1}$), from modes 2 and 3 to mode 1 ($\alpha^*_{23,1}$), from modes 1 and 3 to mode 2 ($\alpha^*_{13,2}$) and finally, from modes 1 and 2 to mode 3 ($\alpha^*_{12,3}$). In the absence of strong cubic non-linearity, the term $\alpha^*_{12,3}\psi_1\psi_2$ will generate, and transfer energy, to mode 3 through a combination resonance (a *heterodyne effect*). This is the third mode mechanism suggested by Achong [1] on the steelpan notes when only quadratic non-linearity is assumed. The cross-terms in equation (21) will all vanish as $H_0 \to 0$.

A general observation on all coefficients $\alpha_{ij,n}$ is that through their dependence on the static state ψ_0, not only is the frequency altered by changes in thermal and compressive stresses but so are the couplings that are second order in the modal co-ordinates.

4.6.3. *Cubic terms*

Of all the cubic coefficients, $\beta_{111,3}$ is singled out for special mention because it determines the generation of an internal resonance at ω_3. All other cubic coefficients are relegated to Appendix B. This coefficient is expressed as

$$\beta_{111,3} = \frac{1}{2}\bar{Z}_3(\psi'_1, \psi'^2_1) - \frac{1}{2}\bar{V}_3(\psi'^3_1). \tag{22}$$

In this expression, the effect of the rise-factor is not immediately obvious (dependence comes only through the effect of the rise factor on the modal co-ordinates ψ_n). In fact, the terms involving the cubic coefficients persist even at the flat plate limit. Compared to the quadratic coefficients, the cubic coefficients (on the pan) are consistently lower in magnitude and this explains why panmakers have always experienced great difficulty in obtaining strong third modes on the instrument.

5. ELLIPSOIDAL NOTES

While the note dynamics can be understood from the present analysis with the restriction to symmetrical motion on a circular planform, greater flexibility in tuning is allowed on notes with elliptical areas of confinement. On an elliptical planform, the second and third natural modes can be more readily tuned to the required harmonic relationship with the first mode by employing modes that are symmetrical with respect to the minor axis and the major axis, respectively.

To deal fully with ellipsoidal shapes, the co-ordinate space must be increased dimensionally. This will yield equations that are much more complicated than those presented here but is worth doing especially for the practical application of the results. This refinement will, however, leave the non-linear form of equation (14) unchanged (see for example, reference [19]). In such an exercise, it would be useful to produce a "semi-general" solution containing the aspect ratio of the planform as an adjustable parameter in the same way that the rise factor appears in the present equations. It would then be possible to avoid performing the numerical solutions on the non-linear equations in order to see, albeit in a qualitative way, how the aspect ratio affects mode couplings.

6. EXPERIMENTAL OBSERVATIONS

6.1. THERMAL EFFECTS ON FREQUENCY SPECTRA

Consider the note in an initial state of zero thermal stress (i.e., the steelpan is at the temperature at which it was initially tuned). The temperature is then increased by δT to move the pan to a final state of thermal stress. Using equation (16) together with the previous definitions for $\breve{N}_T$ and $B(\psi_0)$, for the resulting small frequency shift $\delta\omega$, one obtains

$$\delta\omega_n = -\frac{\alpha\delta T}{2\omega_{i,n}}(1+\nu)\left(\frac{a}{h}\right)^2 \bar{X}_n(\psi_n) - \frac{B_f(\psi_0) - B_i(\psi_0)}{2\omega_{i,n}}, \tag{23}$$

where the subscripts i and f denote initial and final values, respectively.

The first term on the right-hand side of equation (23) represents the effect of the change in dynamic stiffness brought about by the thermal stress, while the second term in ψ_0 represents the effect of the accompanying change in surface

shape. The first term should dominate to produce an approximately linear dependence of frequency shift on temperature change. In addition, the first term predicts that the change in frequency will be proportional to $(a/h)^2$, which means that notes of larger surface area and of thinner material should show greater dependence on temperature. In other words, the bass instruments with their larger notes, should suffer a greater degree of mis-tuning as the pan temperature is varied. For notes on elliptical planforms, to a first approximation (aspect ratios close to unity), a^2 in equation (23) may be replaced by (ab) where a and b are the semi-major and semi-minor axes respectively.

To confirm these theoretical results, steelpans were subjected to temperature changes in the range 23·5 to 57°C, and at each state, the surface velocity data generated by impact were recorded. The experimental method for data collection and handling can be found in reference [1]. Displacement data were computed by integration and spectral data generated by taking the Fourier transform. The frequency modulations [1] associated with the non-linear modal interactions are expected to be much smaller than the thermally/compressively induced shifts in frequency. To reduce estimation errors for the maxima on the spectra, a second-order interpolation function [20] was applied using three frequency-amplitude pairs of values at each peak.

6.1.1. *Tenor*

Figures 4(a) and (b) show the shift in first-mode peaks for the G_4 note (elliptical planform, minor × major axes = 10 × 13 cm) and the D_4 note (elliptical planform: 10·5 × 13 cm) on the tensor. The G_4 note (393·2 Hz at 27·5°C) shifted downward in frequency at a rate of −0·014 Hz/deg to present a −0·1% change in frequency at the final temperature of 54°C. The D_4 note dropped from 293·5 Hz at 27·5°C to 288·2 at 54°C, representing a rate of −0·2 Hz/deg and a frequency change of −1·8%. These rates of frequency decrease with increasing temperature and are typical of the values for notes on other tenor pans.

A secondary result, clearly observable on the spectral data, is the broadening of the peaks as the temperature is increased. Corresponding to this increase in

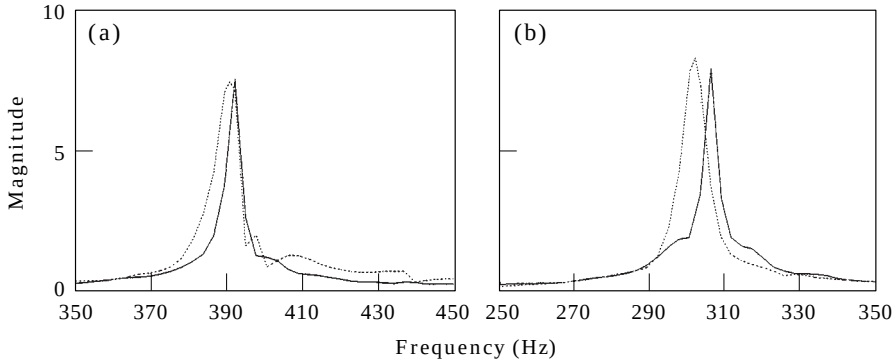

Figure 4. First mode peaks on the tenor for (a) the G_4 note at 27·5°C (—) and at 54°C (- - -); (b) the D_4 note at 27·5°C (—) and at 54°C (- - -).

bandwidth, there occurred a reduction in the duration of the sounded tone for both these notes. This is of importance because it implies an increase in damping as the temperature increases.

6.1.2. *Bass*

Figure 5 shows the complete spectra (below 400 Hz) at 27·5°C (full line) and at 56°C (dotted line) for the $F_2^\sharp$ note (planform minor × major axes = 18 × 27 cm) on a bass pan. On the scale of Figure 5, the peak broadening is unobservable but by plotting the velocity data as in Figure 6 one can observe the increase in duration from the longer persistence of the vibrations at the lower temperature. Also, by comparing the two plots in Figure 6, one can see the changes to the modulated velocity envelopes resulting from the effect of a change in temperature on the modal coupling. The effect of temperature on the damping of these shell structures is the subject of further study.

In Figure 5, the first mode peak labelled b, at 92·40 Hz is shifted downward (peak a) to 84·34 Hz. This represents a rate of −0·28 Hz/deg or a frequency change of −8·7%. The second mode peak e (191·19 Hz), is shifted down to c (177·57 Hz) for a change of −7·1%. The third mode g (284·67 Hz) is shifted down to f (261·35 Hz) for a change of −8·2%.

The peak labelled d (184·60 Hz) on the 27·5°C data, corresponds to the parametrically generated vibration controlled by the quadratic coupling coefficient $\alpha_{11,2}$. This non-linear mode will be observed with small detuning [1], close to $2\omega_1$ ($\equiv 2 \times 92{\cdot}40 = 184{\cdot}80$ Hz). At 56°C, the corresponding parametric mode is not observable, indicating a possible reduction in $\alpha_{11,2}$. The cubic parametric modes are unobservable at both temperatures. Notice, however, the appearance at 56°C of a fourth mode h, at 354·14 Hz, very likely a normal mode as the frequency is not close to multiples of the first mode frequency or any linear combination of lower frequences.

The second mode to first mode frequency ratio on the $F_2^\sharp$ note increases from 2·069 at 27·5°C to 2·105 at 56°C. Closer harmonicity would be required were this

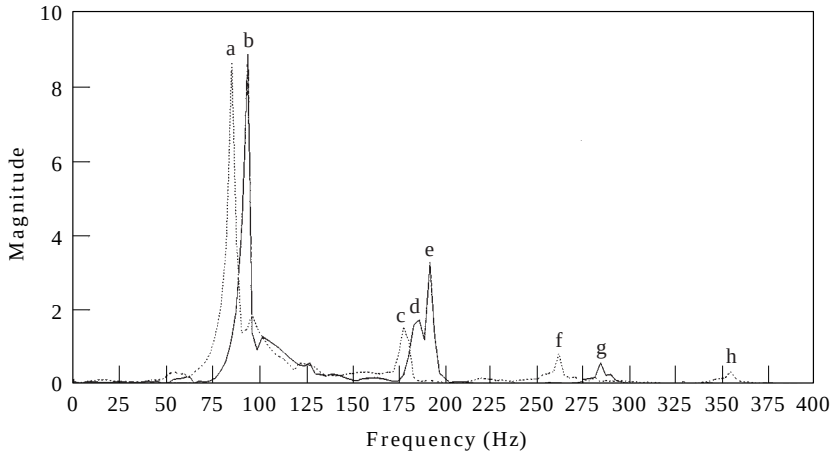

Figure 5. Spectra for the $F_2^\sharp$ bass note at 27·5°C (—) and at 56°C (- - -).

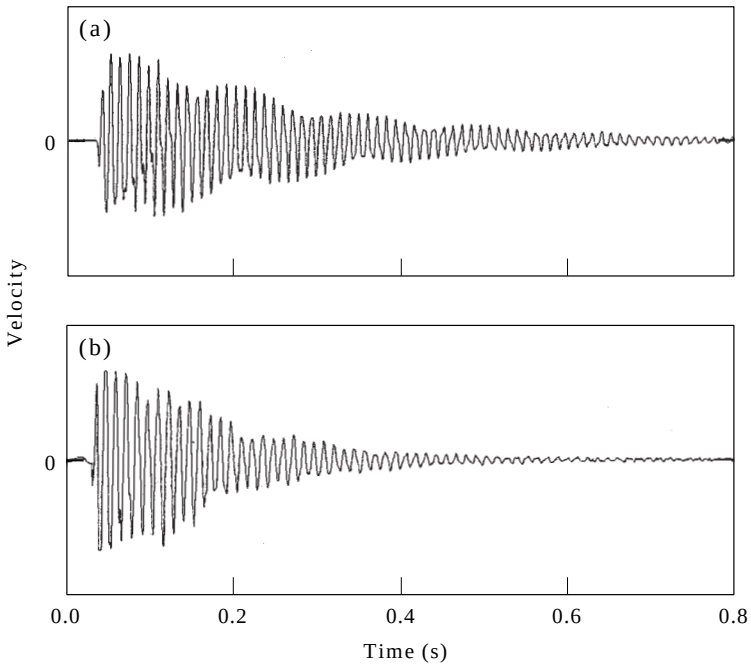

Figure 6. Velocity–time graphs for the $F_2^{\sharp}$ bass note (a) at 27·5°C and (b) at 56°C.

a note on a higher frequency pan, such as the tenor. The present note displays a relatively weak second mode because the lack of close harmonicity results in a reduction in energy transferred between first and second modes. In any event, dominating second modes are not required on the bass.

These observations are all consistent with equation (23) with the percentage frequency shifts on the bass consistently higher than those on the tenor. Direct comparison with the product (*ab*) is not possible because of the factor $\bar{X}_n(\psi_n)$ which is dependent on the shape and boundary conditions (unknown) of the particular note. For these ellipsoidal notes, $\bar{X}_n(\psi_n)$ will also take on a more general form.

6.1.3. *Cello*

Similar observations were made on a steelpan cello at temperatures of 23·5, 34·5, 44, 50·0 and 57°C. This particular pan was selected not on the basis of tonal qualities but rather to show the appearance of parametric excitations. On a well tuned pan with good tonal qualities, because of the small degree of detuning (close harmonicity), the spectral peaks for these excitations would have merged too closely with the peaks for the normal modes. The results are shown in Figures 7(a) to (f) for the E_3^b note, where, for clarity, only the data at 23·5, 44 and 57°C are shown on the spectral plots. The frequency versus temperature plots show some departure from linearity expected from the first term on the right-handside of equation (23). This shows the importance of the second term

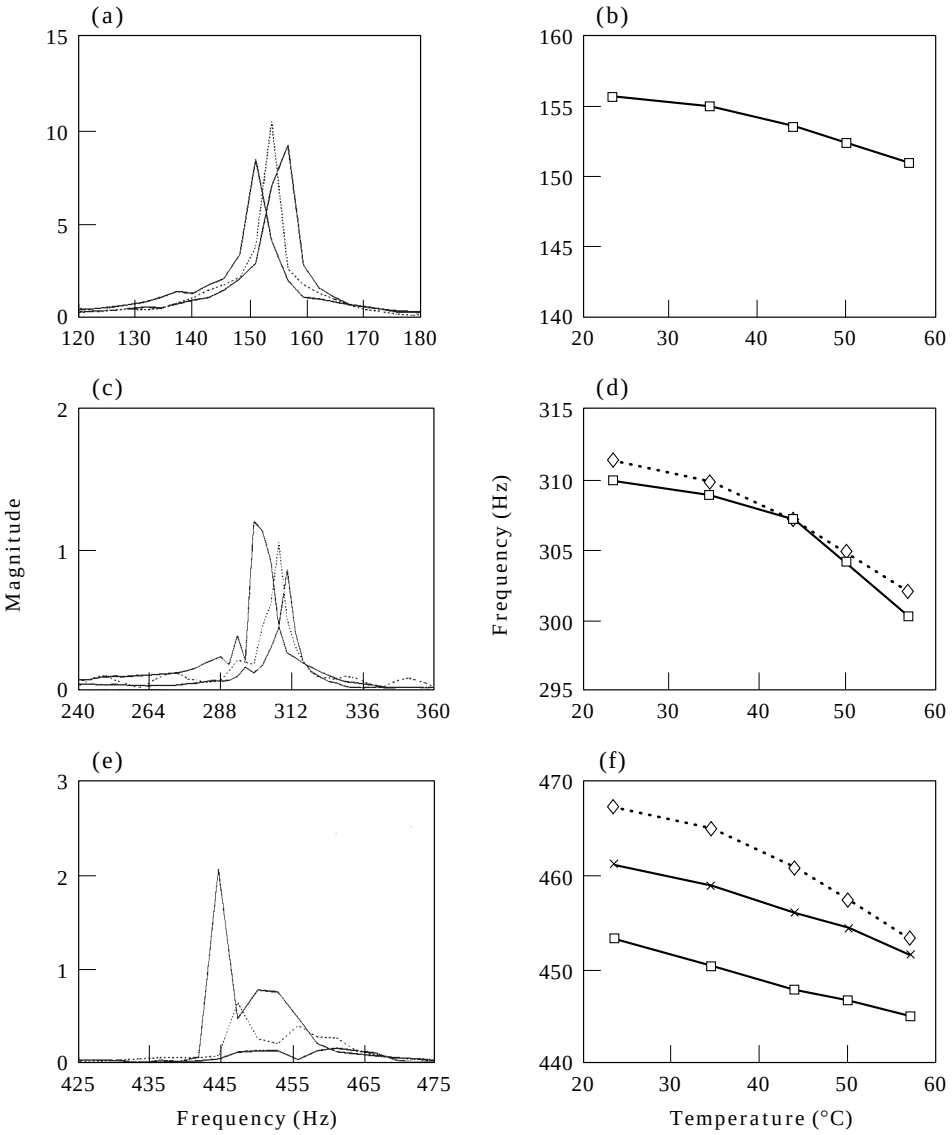

Figure 7. The E_3^b note on the cello;. (a), (c) and (e) first, second and third normal mode peaks, respectively, at 23·5, 44 and 57°C. (b), (d) and (f) show the complete frequency–temperature plots. Dotted lines in (d) and (f) are the plots of $2f_1$ and $3f_1$, respectively. Points marked by $\times$ in (f) are the parametric excitations represented by the higher frequency components of the double peaks in (e).

of this equation which contains the effects on frequency of temperature induced changes to the mode shape.

In Figure 7(e), double peaks appear for the third modes. The lower frequency peak on each plot represents the normal mode while the higher frequency peak represents the parametric excitation at $3f_1$ resulting from the cubic non-linearity. In Figure 7(f) a plot of the expected frequencies of the parametric excitations (dotted curve) is shown. Notice that the amplitudes of all the peaks in Figure 7(e) grow with increasing temperature. Parametric excitations due to quadratic

non-linearities are not observable on the spectral data in Figure 7(c), due possibly to merging or to low levels of excitation.

6.2. THE TRANSITION PERIOD BETWEEN FIRST AND SECOND TUNING

Immediately after "first tuning", the instrument goes through a rather complex metallurgic/dynamic process as the stresses are relieved and redistributed resulting in changes to the modal frequencies, the coupling coefficients and the surface shape. Using equation (16) together with the previous definitions for $\breve{N}_c$ and $B(\psi_0)$, for a small increase in the compression δN_c, one obtains the frequency shift

$$\delta\omega_n = -\frac{\delta N_c(1-\nu^2)a^2}{2\omega_{i,n}Eh^3}\bar{X}_n(\psi_n) - \frac{B_f(\psi_0) - B_i(\psi_0)}{2\omega_{i,n}}. \tag{24}$$

One sees from equation (24), that larger notes or notes of thinner material would be more susceptible to the effects of stress relaxation during the transition period that follows tuning.

The sequence of changes during stress relaxation is unique to each note on a pan. However, the results presented for the sample note will be typical of most notes. Observations were made on a newly constructed tenor pan immediately after first tuning and then later, after being kept at an approximately constant temperature of 23°C for 24 h. The shift in the spectral peaks corresponding to first, second and third modes for the E_4^b note are shown in Figures 8(a) to (c), respectively.

In Figure 8(a), the first mode shows a shift upwards from its initial frequency of $f_1 = 314{\cdot}84$ Hz (peak 1) to $d_1^* = 317{\cdot}68$ Hz (peak 2), a shift of $+2{\cdot}84$ Hz. In Figure 8(b) the second mode natural frequency (peaks 3 and 4, respectively) shows a shift from $f_2 = 609{\cdot}59$ Hz to $f_2^* = 610{\cdot}55$ Hz (a shift of $+0{\cdot}96$ Hz). The peak labelled 5, at 629·94 Hz, corresponds to the slightly detuned parametrically excited mode expected at $2f_1$ ($=629{\cdot}68$ Hz). Twenty-four hours later, this parametric mode is observed at peak 6 (637·94 Hz), now much more detuned from the value of $2f_1^*$ ($=635{\cdot}36$ Hz). The sign (direction) of these frequency shifts indicate a reduction in compressive stress ($\delta N_c < 0$) consistent with stress relaxation.

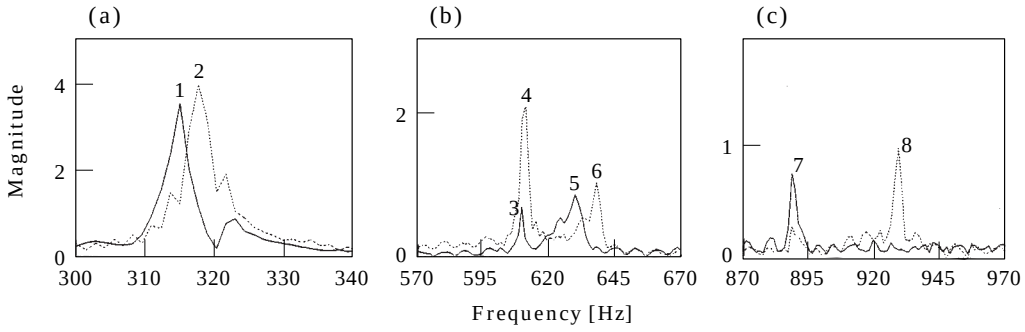

Figure 8. The effects of stress relaxation on the frequency components E_4^b of the tenor note; —, before relaxation; - - -, after relaxation. (a) First mode showing an upward shift after relaxation; (b) changes to both the second normal modes (peaks 3 and 4) and the parametric excitations (peaks 5 and 6); (c) shift in frequency of third normal modes.

In Figure 8(c), the frequency for the third natural mode moved from $f_3 = 888{\cdot}62$ Hz (peak 7) to $f_3^* = 928{\cdot}58$ Hz (peak 8). This large shift may be related to sensitive dependence on this particular note to changes in surface shape (through the connection of ψ_0 to the compressive stress). No parametric excitation resulting from cubic non-linearities is observable.

7. CONCLUSION

The present work provides the structural analysis lacking in references [1–3] where, for example, it was shown that all the first and second mode modulation features observed on the notes of the steelpan can be synthesized by a non-linear model involving internal (quadratic) resonances. The effects of thermally or compressively induced stresses on frequencies and coupling coefficients have been demonstrated. By carefully developing the non-linear equations in the present work, numerical solutions were not required, instead, qualitative results were obtained directly from the terms in the equations. This was particularly useful because one has no direct access to or knowledge of the values for the elastic spring constants (K and C) that determine the boundary conditions for the shell structures.

The analytical and experimental work both showed the existence of parametrically excited modes in addition to the normal modes, providing the means for internal resonances. Perhaps the most convincing demonstration of the presence of internal resonances on this instrument comes during the tuning process itself. The moment that the tuner has correctly shaped a note and set the right conditions (boundary and in-plane stresses) by peening, the note "sings" loudly with a beautiful resonance. This is the moment when the modes are set into a nearly perfect harmonic relationship.

REFERENCES

1. A. ACHONG 1996 *Journal of Sound and Vibration* **197**, 471–487. The steelpan as a system of non-linear mode-localized oscillators, part I: theory, simulations, experiments and bifurcations.
2. A. ACHONG and K. A. SINANAN-SINGH 1997 *Journal of Sound and Vibration* **203**, 547–561. The steelpan as a system of non-linear mode-localized oscillators, part II: coupled sub-systems, simulations and experiments.
3. A. ACHONG 1998 *Journal of Sound and Vibration* **212**, 623–635. The steelpan as a system of non-linear mode-localized oscillators, part III: the inverse problem—parameter estimation.
4. Y.-Y. YU 1963 *Journal of Applied Mechanics* **30**, 79–86. Application of variational equation of motion to the non-linear vibration analysis of homogeneous and layered plates and shells.
5. D. A. EVENSEN 1963 *American Institute of Aeronautics Astronautics Journal* **1**, 2857–2858. Some observations on the nonlinear vibration of thin cylindrical shells.
6. P. L. GROSSMAN, B. KOPLIK and Y.-Y. YU 1969 *Transactions of the American Society of Mechanical Engineers Journal of Applied Mechanics* **39E**, 451–458. Nonlinear vibrations of shallow spherical shells.
7. A. NIKU-LARI 1981 in *First International Conference on Shot Peening* (A. Niku-Lari, editor) 1–21. Oxford: Pergamon Press. Shot peening.

8. W. JOHNSON 1982 in *Mechanics of Solids* (H. G. Hopkins and M. J. Sewell, editors) 303–356. Oxford: Pergamon Press. The mechanics of some industrial pressing, rolling, and forging processes.
9. A. ACHONG 1997 *NIHERST Sci-TechKnoFest* 97. The steelpan: theory of operation (presented to: NIHERST, National Institute of Higher Education Science and Technology).
10. A. ACHONG 1998 *Journal of Sound and Vibration* **191**, 207–217. Vibrational analysis of mass loaded plates and shells by the receptance method with application to the steelpan.
11. M. E. KING and VAKAKIS 1996 *Transactions of the American Society of Mechanical Engineers Journal of Applied Mechanics* **63**, 810–819. An energy-based approach to computing resonant nonlinear normal modes.
12. J. CONNOR, JR. 1962 *NASA TH B*1510, 623–642. Nonlinear transverse axisymmetric vibrations of shallow spherical shells.
13. R. R. ARCHER 1962 *American Society of Mechanical Engineers Journal of Applied Mechanics* **29**, 502–505. On the influence of uniform stress states on the natural frequencies of spherical shells.
14. B. A. BOLEY and J. H. WEINER 1960 *Theory of Thermal Stresses*. New York: Wiley.
15. A. H. NAYFEH 1973 *Perturbation Methods*. New York, Wiley.
16. J. KEVORKIAN 1987 *Society for Industrial and Applied Mathematics Review* **29**, 391–462. Perturbation techniques for oscillatory systems with slowly varying coefficients.
17. M. W. WILCOX and L. E. CLEMMER 1964 *Proceedings of the American Society of Civil Engineers Journal of Engineering. Mechanics Division* **90**, 165–189. Large deflection analysis of heated plates.
18. L. KOLLÁR and E. DULÁESKA 1984 *Buckling of Shells for Engineers*. New York: Wiley.
19. K. YASUDA, K. KAMIYA and M. KOMAKINE 1997 *Transactions of the American Soclety of Mechanical Engineers Journal of Applied Mechanics* **64**, 275–280. Experimental identification technique of vibrating structures with geometrical nonlinearity.
20. S. ANDO and K. YAMAGUCHI 1993 *Journal of the Acoustical Society of America* **94**, 37–45. Statistical study of spectral parameters in musical instrument tones.

APPENDIX A: DEFINITION OF FUNCTIONALS

The following functionals in the form G ($variable_1$, $variable_2, \ldots$) are defined (double integrals are the result of solving for u in equation (10b)):

$$L(A) = \nabla^4 A, \quad M(A) = A, \tag{A1, 2}$$

$$P(A, B) = \left[\left(\frac{\mathrm{d}}{\mathrm{d}x} + \frac{1}{x}\right)\left(\frac{1}{x}\int_0^x \left(\int_0^x A\ \mathrm{d}x\right) x\ \mathrm{d}x - x\left[\int_0^x \left(\int_0^x A\ \mathrm{d}x\right) x\ \mathrm{d}x\right]_{x=1}\right)\right] B, \tag{A3}$$

$$S(A, B) = \left[\left(\frac{\mathrm{d}}{\mathrm{d}x} + \frac{1}{x}\right)\left(\frac{1}{x}\int_0^x \left(\int_0^x \left(\frac{\mathrm{d}}{\mathrm{d}x} + \frac{1-\nu}{x}\right) A\ \mathrm{d}x\right) x\ \mathrm{d}x - x\left[\int_0^x \left(\int_0^x \left(\frac{\mathrm{d}}{\mathrm{d}x} + \frac{1-\nu}{x}\right) A\ \mathrm{d}x\right) x\ \mathrm{d}x\right]_{x=1}\right)\right] B, \tag{A4}$$

$$V(A) = \left[\left(\frac{\mathrm{d}}{\mathrm{d}x} + \frac{1}{x}\right)A\right], \quad X(A) = -\nabla^2 A, \tag{A5, 6}$$

$$Y(A, B) = \left(\frac{\mathrm{d}}{\mathrm{d}x} + \frac{1}{x}\right)\left(A\left(\frac{\mathrm{d}}{\mathrm{d}x} + \frac{\nu}{\mathrm{d}x}\right)\left(\frac{1}{x}\int_0^x \left(\int_0^x B\,\mathrm{d}x\right)x\,\mathrm{d}x - x\left[\int_0^x \left(\int_0^x B\,\mathrm{d}x\right)x\,\mathrm{d}x\right]_{x=1}\right)\right), \tag{A7}$$

$$Z(A, B) = \left(\frac{\mathrm{d}}{\mathrm{d}x} + \frac{1}{x}\right)\left(A\left(\frac{\mathrm{d}}{\mathrm{d}x} + \frac{\nu}{x}\right)\left(\frac{1}{x}\int_0^x \left(\int_0^x \left(\frac{\mathrm{d}}{\mathrm{d}x} + \frac{1-\nu}{x}\right)B\,\mathrm{d}x\right)x\,\mathrm{d}x - x\left[\int_0^x \left(\int_0^x \left(\frac{\mathrm{d}}{\mathrm{d}x} + \frac{1-\nu}{x}\right)B\,\mathrm{d}x\right)x\,\mathrm{d}x\right]_{x=1}\right)\right). \tag{A8}$$

The Galerkin averaging performed over the nth mode gives a set of averaged functionals as illustrated for the generic functional G:

$$\bar{G}_n(var_1, \ldots) = \frac{\int_0^1 G(var_1, \ldots)\psi_n x\,\mathrm{d}x}{\int_0^1 \psi_n^2 x\,\mathrm{d}x}. \tag{A9}$$

APPENDIX B: CUBIC COUPLING COEFFICIENTS

In mode 1 the coefficients for the terms $\beta^*_{113,1}w_1^2 w_3$ and $\beta^*_{223,1}w_2^2 w_3$ are given by

$$\beta^*_{jj3,1} = \bar{Z}_1(\psi'_j, \psi'_j\psi'_3) + \frac{1}{2}\bar{Z}_1(\psi'_3, \psi_j'^2) - \frac{3}{2}\bar{V}_1(\psi_j'^2\psi'_3), \quad (j = 1, 2). \tag{B1}$$

The coefficient $\beta^*_{123,2}$, for the cubic term $\beta^*_{123,2}w_1 w_2 w_3$ in mode 2 is given by

$$\beta^*_{123,2} = \bar{Z}_2(\psi'_1, \psi'_2\psi'_3) + \bar{Z}_2(\psi'_2, \psi'_1\psi'_3) + \bar{Z}_2(\psi'_3, \psi'_1\psi'_2) - 3\bar{V}_2(\psi'_1\psi'_2\psi'_3). \tag{B2}$$

Finally, in mode 3, and corresponding to the term $\beta^*_{122,3}w_1 w_2^2$, is the coefficient

$$\beta^*_{122,3} = \bar{Z}_3(\psi'_2, \psi'_1\psi'_2) + \frac{1}{2}\bar{Z}_3(\psi'_1, \psi_2'^2) - \frac{3}{2}\bar{V}_3(\psi'_1\psi_2'^2). \tag{B3}$$